



Characterization, adsorption isotherm, and kinetic of mesoporous silica microspheres for dyeing wastewater

Jiawei Cui, Guanghui Wang, Chao Wang, Ping Ke, Qi Tian, Yongsheng Tian*

Hubei Coal Conversion and New Carbon Materials Key Laboratory, School of Chemistry and Chemical Engineering, Wuhan University of Science and Technology, 430081 Wuhan, China, Tel. +86-13164631033; email: wkdt_tys@126.com (Y. Tian), Tel. +86-18671050527, email: cuijiawei_WUST@163.com (J. Cui), Tel. +86-13507112902, email: wghwang@263.net (G. Wang), Tel. +86-15671683285; email: 1638646037@qq.com (C. Wang), Tel. +86-13164631022; email: keping_WUST@163.com (P. Ke), Tel. +86-15072344500; email: 769199902@qq.com (Q. Tian)

Received 3 July 2020; Accepted 5 December 2020

ABSTRACT

A simple process for the preparation of mesoporous silica microsphere (MSM) as adsorbent was synthesized via sol-gel method between tetraethyl orthosilicate and polyethylene oxide-polypropylene oxide-polyethylene oxide (F127). The influencing factors of MSM on methyl orange simulated dyeing wastewater were investigated in detail. Five adsorption isotherm models, kinetics, thermodynamics, and mechanism were studied. Under the optimum conditions, the adsorption rate was up to 86.44% (only at 21 min). The adsorption process of methyl orange by MSM was indicated as a non-spontaneous monolayer chemical adsorption process, which obeyed the pseudo-second-order kinetic model. The above showed that the MSM as-prepared in this paper was a simple, efficient and promising adsorbent for wastewater treatment, which provided a theoretical basis and technical support for the dyeing wastewater treatment.

Keywords: Mesoporous silica; Dyeing wastewater; Adsorption isotherm; Kinetics

1. Introduction

With the rapid development of the textile industry, a large amount of dyeing wastewater with strong colority [1], degradation resistance [2], high toxicity [3] is discharged into rivers, which has become an important cause of water pollution, resulting in great harm to the environmental and human health. At present, dyeing wastewater is considered as one of the key points of industrial wastewater treatment and has drawn great public concerns. In recent years, various methods have been applied to the purification and remediation of dyeing wastewater, such as membrane filtration [4], oxidation [5], biodegradation [6], and adsorption [7]. Adsorption is considered to be an effective and economical method for dyeing wastewater treatment due to its significant advantages of low cost, simple

design and high efficiency [8,9], compared with the other approaches. Up to now, a variety of absorbents [10–15] have been studied and utilized in wastewater treatment, such as clay, resins, proteins, activated carbon, etc. However, its industrial applications have been limited because of the disadvantage of complex preparation and poor efficiency. Therefore, it is of great significance to choose a simple and efficient adsorbent for dyeing wastewater treatment.

Materials are generally divided into microporous, mesoporous, and macroporous materials. Whereas the microporous materials with small pore size make it difficult for macromolecules to enter or exit the channels, and the macroporous materials with wide pore size distribution limited its industrial applications. Thus, mesoporous materials (pore diameters of 2–50 nm) have been universally used in

* Corresponding author.

targeted drugs [16], catalyst loading [17], protein immobilization [18] and decolorization [19,20] researches with its adjustable pore size, large surface area, strong hydrothermal stability, and stable skeleton structure. As a typical mesoporous material, mesoporous silica has the characteristics of great biocompatibility and environmental friendliness [21], besides the advantages of mesoporous materials. It naturally has become the research focus for dyeing wastewater treatment. Nevertheless, due to its limited ion exchange capacity and the harshness of the synthesis conditions, conventional mesoporous silica cannot meet people's expected requirements. Therefore, researchers have been trying to synthesize mesoporous silica in a variety of simple and fast ways to change its original physical and chemical properties to meet dyeing wastewater treatment needs.

The purpose of this paper is to develop a simple, efficient and promising adsorbent for wastewater treatment. Mesoporous silica microsphere (MSM) was synthesized by sol-gel method using tetraethyl orthosilicate (TEOS) and poly(ethylene oxide)-poly(propylene oxide)-poly(ethylene oxide) (F127). The adsorption performance of MSM as an adsorbent for methyl orange simulated dye wastewater was investigated. The effects of pH value, MSM dosage, temperature and time on the adsorption effect were studied. The adsorption isotherm model, adsorption kinetics, adsorption thermodynamics and mechanism of the adsorption process were discussed in detail.

2. Materials and methods

2.1. Materials

F127 was purchased from Sigma-Aldrich LLC, (USA). The other chemicals including TEOS, ethanol, ammonia, hydrochloric acid (HCl), sodium hydroxide (NaOH), were purchased from Sinopharm Chemical Reagent Co., Ltd., (Shanghai, China). All reagents were of analytical grade and no further purification was required. The pH of aqueous solutions was controlled by adding appropriate amounts of HCl or NaOH.

2.2. Preparation of MSM

The MSM was prepared by hydrolysis of TEOS in an alcohol-water mixed solvent using F127 as template. 0.30 g F127 was dissolved in a certain amount absolute ethanol-ammonia mixed solution and stirred to obtain a microemulsion system. Then, TEOS was added dropwise to the prepared microemulsion system with stirring to dissolve, subsequently let it stand for crystallization. After crystallization was completed, the crystallization solution was dried in a vacuum oven at 80°C. Finally, MSM was obtained by calcining dried powder in a muffle furnace.

2.3. Drawing of methyl orange standard curve

0.10 g methyl orange was added to distilled water to prepare methyl orange standard solutions with concentrations of 1.0, 1.5, 2.0, 2.5, 3.0, 3.5, 4.0, and 4.5 mg/L. Subsequently, the absorbance at a wavelength of 463 nm was measured with an ultraviolet spectrophotometer. The methyl orange concentration and the absorbance were plotted on the abscissa and the ordinate, respectively,

which methyl orange standard curve is shown in Fig. 1. It can be clearly seen that the adsorption curve of methyl orange was linearly related. The standard curve of methyl orange was drawn before each running to guarantee the stability and accuracy of each experiment.

2.4. Adsorption experiments

0.20 g MSM and a certain concentration of methyl orange solution were mixed in a 50 mL Erlenmeyer flask, following shaken on a constant temperature oscillator of 35°C. The sample was measured by the absorbance of the solution at a wavelength of 463 nm, and the adsorption rate R (%) was calculated according to the following formula [22]:

$$R = \frac{C_0 - C_t}{C_0} \times 100\% \quad (1)$$

where C_0 (mg/L) and C_t (mg/L) are the concentration of methyl orange before and after adsorption, which are obtained by the absorbance.

2.5. Characterization

The morphology of the microspheres nanoparticles was observed using scanning electron microscopy (SEM, FEI Nova 400 Nano) with a working voltage of 15 kV. Fourier-transform infrared spectroscopy (FT-IR) spectra (4,000–500 cm^{-1}) were recorded at room temperature on a Bruker VERTEX 70 (Germany) FT-IR spectrometer using KBr in the ratio of 1:200. The X-ray diffraction (XRD) patterns were recorded on a Phillips Xpert Pro powder diffraction (Holland) system using Cu K α radiation with a Ni filter over the range $10^\circ \leq 2\theta \leq 80^\circ$. The surface area analyzer (Autosorb-1-C) from American Kangta Company outgassed more than 6 h at 200°C under vacuum before measurement. Ultraviolet-visible Spectrophotometer was performed by a CARY 300 instrument from an American Agilent company.

3. Results and discussion

3.1. Characterization of MSM

The morphology of the as-prepared MSM is shown in Fig. 2. It can be seen that the sample exhibited microsphere

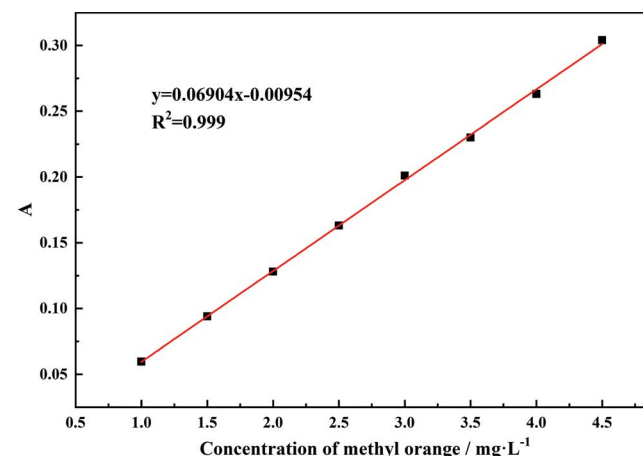


Fig. 1. Standard curve of methyl orange.

particles shape with relatively uniform size, and the particle size of 400–600 nm.

FT-IR spectra of MSM before and after calcination are shown in Fig. 3. As can be seen that the broad band around $3,430\text{ cm}^{-1}$ was attributed to the stretching vibration peaks of Si–OH. The characteristic band observed in the FT-IR spectrum at $1,071$ and 794 cm^{-1} were assigned to the stretching vibration peak of Si–O–Si [23]. The absorption band at 960 cm^{-1} can be ascribed to the vibration of Si–OH bond. The characteristic band at 470 cm^{-1} was designated to the fundamental vibrational modes of Si. All the above indicated that the MSM was successfully prepared by the sol–gel method with F127 as template. Comparing with the MSM before calcination, it can be observed that the characteristic band around $2,925\text{--}2,860\text{ cm}^{-1}$ corresponding to the stretching vibration peak of C–H disappeared after calcination, showing that the templating agent was successfully removed after calcination.

The XRD pattern of samples is shown in Fig. 4. It can be seen that the sample before calcined appeared a distinct

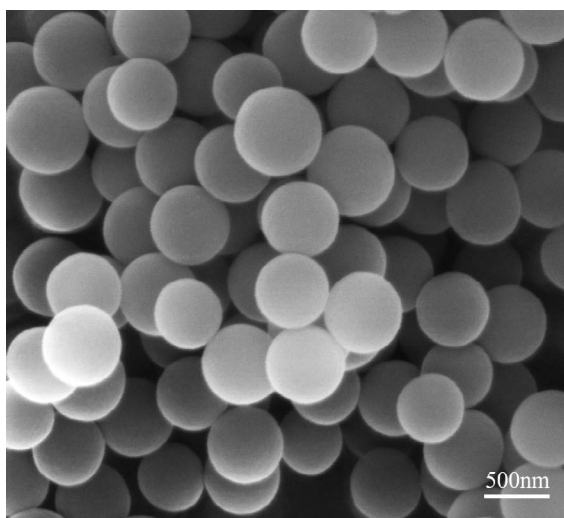


Fig. 2. SEM micrograph of MSM.

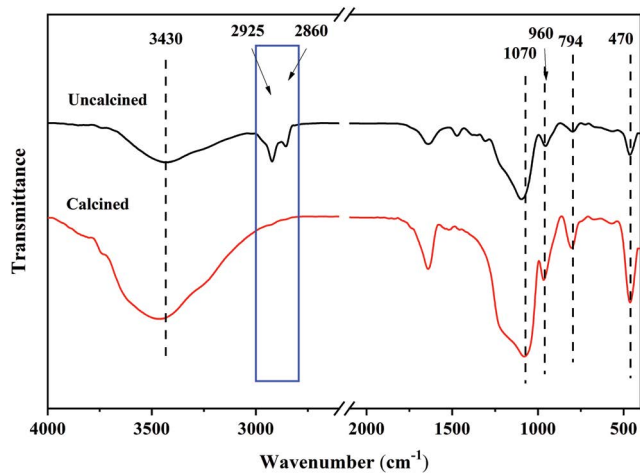


Fig. 3. FT-IR spectra of MSM.

characteristic peak at $2\theta = 18.5^\circ$, which was indexed as the diffraction of carbon. Nevertheless, the calcined sample without any distinct characteristic peaks, indicating that the as-prepared MSM had an amorphous structure and the template was well removed.

The N_2 adsorption–desorption curve of MSM is assayed in Fig. 5, and its pore structure analysis is listed in Table 1. As seen, the N_2 adsorption–desorption curve of MSM belonged to the typical IV curve with a high hysteresis loop of H_2 type, indicating that the MSM had a cage-shaped mesoporous channel. Additionally, the MSM exhibited a large surface area ($326.08\text{ m}^2/\text{g}$), and the pore diameter of 14.67 nm , showing an obvious mesoporous structure, which was conducive to the adsorption of macromolecular dyes.

3.2. Effects of conditions on adsorption

The effects of pH, dosage of MSM, temperature, and time on the adsorption efficiency are shown in Fig. 6. It was found that different adsorption conditions showed a great influence on the adsorption efficiency.

It was examined from Fig. 6a that the adsorption efficiency and the pH value were closely related. The adsorption

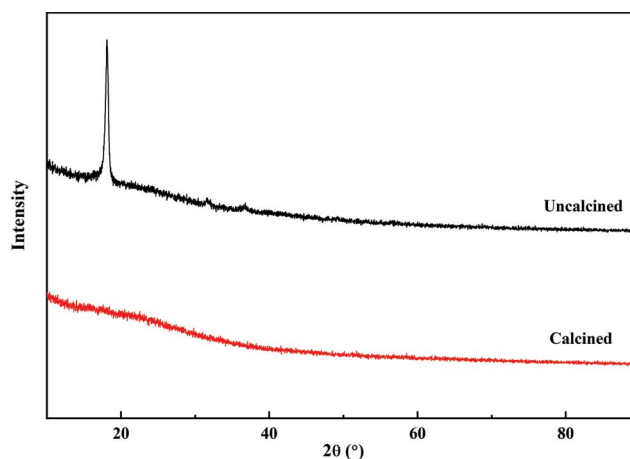


Fig. 4. XRD spectra of mesoporous silica microspheres.

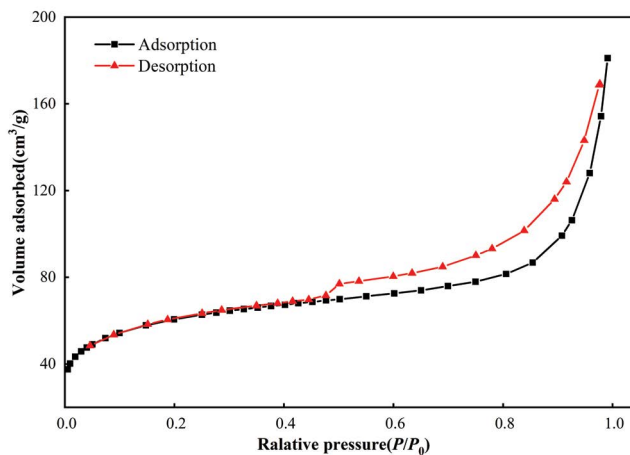


Fig. 5. Adsorption–desorption curve of MSM.

efficiency decreased as pH value ascended. In the alkaline solution, the adsorption rate was very different from that of the acid solution, showing an obvious poor adsorption efficiency. The above phenomenon was caused by the dissociation of Si–OH in MSM. In a lower pH condition, the positively charged Si–OH in MSM and SO₃⁻ in methyl orange showed electrostatic attraction, which was conducive to the methyl orange adsorption. With the increase of pH, especially in alkaline solution, Si–OH in MSM dissociated into Si–O, which made the surface of MSM negatively charged, and exhibited electrostatic repulsion with SO₃⁻ in methyl orange. When pH = 1, the adsorption rate reached the highest of 80.26%. Thus, the optimal pH value was selected 1.

It can be observed from Fig. 6b that the adsorption rate of methyl orange gradually increased and then tend to be gentle, with an increase of dosage of adsorbent. When the dosage of adsorbent was 0.25 g, the adsorption rate reached 86.44%. However, the adsorption rate remained almost constant when the dosage exceeded 0.25 g. As is to know that with the increase of adsorbent dosage, the adsorption area

of the mesoporous materials will increase, making the active sites adsorbed in the solution subsequently increase, resulting in a gradual increase in the adsorption rate. However, the added excess adsorbent would cause it to overlap each other, and the adsorption sites would also cover or unite with each other, thereby suppressing the increase in the adsorption rate as well as made it tend to be stable [24]. Thus, the optimal dosage selected in this paper as 0.25 g.

The effect of temperature is presented in Fig. 6c. The adsorption rate of methyl orange increased with the temperature increasing, indicating that the adsorption process was endothermic. The molecular motion was not intense at the lower temperature, resulting in poor adsorption efficiency; as the temperature increased, the thermal motion was significantly increased, which was conducive to improving the adsorption process. When the temperature raised to 40°C, the adsorption rate reached a maximum of 86.44%; it maintained constant with the increase of the temperature, showing that the perfect temperature was 40°C.

The effect of adsorption time on the decolorization of dyeing wastewater is shown in Fig. 6d. The adsorption rate was 26.07% with a fast adsorption velocity at 1 min. As the adsorption time increasing, the adsorption velocity gradually decreased. When the adsorption time exceeded 21 min, and the adsorption velocity changed very slowly, making the adsorption rate tend to be gentle. It could be considered that the original number of adsorption points was large, and the driving force for adsorption was increased.

Table 1

Pore structure parameters of MSM

Pore size (nm)	14.67
Surface area (m ² /g)	326.08
Pore volume (cm ³ /g)	1.259

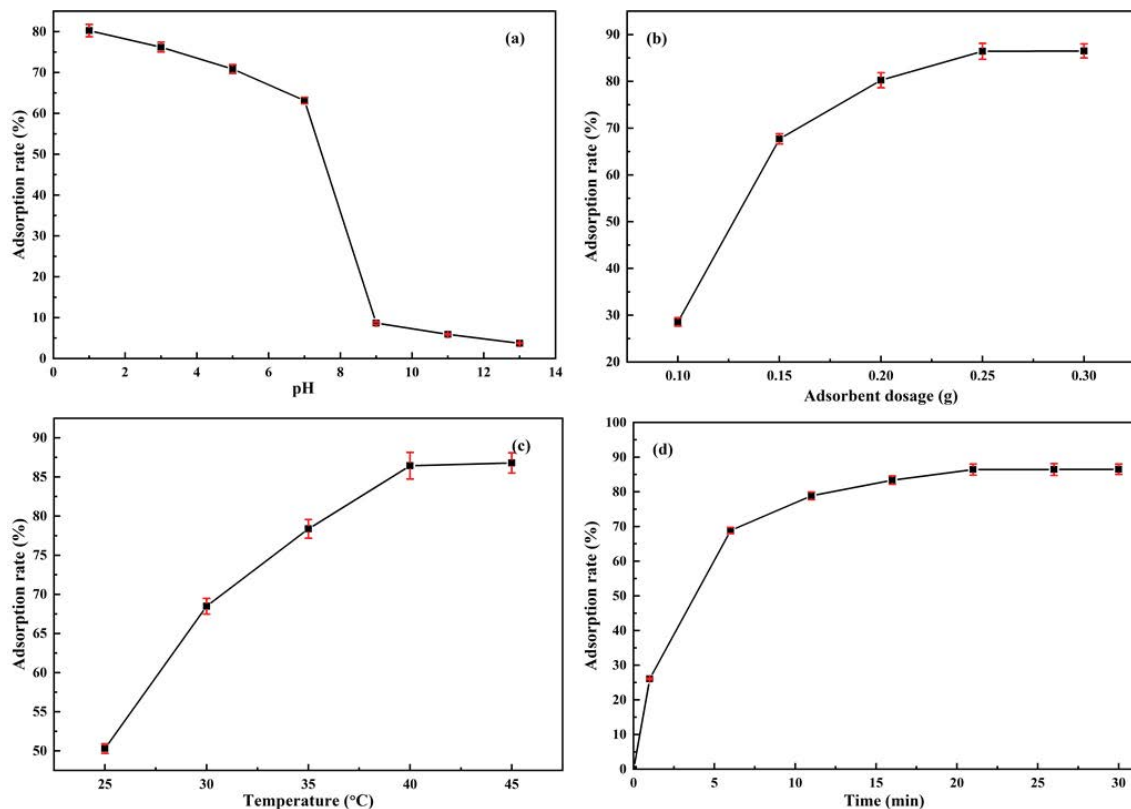


Fig. 6. Effects of different conditions on adsorption. (Experimental conditions: (a) $m(\text{MSM}) = 0.20 \text{ g}$; 21 min; 40°C; (b) pH = 1; 21 min; 40°C, (c) $m(\text{MSM}) = 0.25 \text{ g}$; pH = 1; 21 min, and (d) $m(\text{MSM}) = 0.25 \text{ g}$; pH = 1; 40°C).

As the adsorption time increased, the number of adsorption points gradually decreased, made the accumulation of adsorbate molecules inside the particles increased, which hindered the further movement of the adsorbate molecules. Considering comprehensively the influence of adsorption time on adsorption rate and operating cost, the optimal adsorption time was selected 21 min, at which time the adsorption rate reached 86.44%.

To compare the removal efficiency of MSM to methyl orange dye with other reported adsorbents, and the results are shown in Table 2. The adsorption time of dye is also shown in Table 2 for each adsorbent. It can be clearly seen that the removal efficiency of MSM adsorbent used in this study was rather higher in a shorter time (21 min), compared with other studies. Therefore, MSM in this case can be used as an efficient adsorbent for treating dye-containing solutions.

3.3. Kinetics analysis

3.3.1. Adsorption isotherm

Henry, Langmuir, Freundlich, Temkin and Dubinin–Radushkevich adsorption isotherms were made based on the above experimental. 0.25 g MSM was added to a 50 mL conical flask of methyl orange with a series difference concentration at 40°C. The results are shown in Fig. 7, and the linear forms of the adsorption isotherms equations are summarized in Table 3 [30].

where q_e (mg/g) is the adsorbed amount; C_e (mg/L) is the adsorbate concentrations at equilibrium; ε (kJ/mol) is the adsorption potential based on the Polanyi's potential theory, and the equation is as follows [31]:

$$\varepsilon = RT \ln \frac{C_s}{C_e} \quad (2)$$

It can be seen from Fig. 7 and Table 3 that the Langmuir isotherm model best described the adsorption data, and its fitting coefficient for the MSM adsorption of methyl orange was $R^2 = 0.995$, which was higher than that of the other four adsorption isotherm models. The above phenomenon can be clarified by the fact that the adsorption process of MSM for methyl orange conformed to the Langmuir

adsorption isotherm model, the adsorption process with single-molecular layer adsorption. Additionally, the adsorption of methyl orange by MSM can be inferred as favorable adsorption by estimating the separation factor constant (R_L) of the Langmuir isotherm model and the “ n ” of the Freundlich isotherm model [30,32,33]. Besides, the mean sorption energy E (kJ/mol) can be calculated by the equation $E = \frac{1}{\sqrt{2K_{D-R}}}$, and it was calculated as $E = 8.257$ kJ/mol.

According to $8 < E < 16$ kJ/mol, it can be universally considered that the adsorption is controlled by a chemical process, while $E < 8$ kJ/mol, the adsorption is controlled by a physical process [34–36]. Thus, the adsorption of methyl orange by MSM in this paper can be inferred as a single-molecular layer favorable chemical adsorption process.

3.3.2. Adsorption kinetics

In order to investigate the adsorption mechanism of MSM to methyl orange, quasi-first-order kinetic equation and quasi-second-order kinetic equation were used for regression fitting based on the experimental. The special attention that the premise of the quasi-first-order kinetic equation was that the rate of adsorbate attachment to the

Table 3
Adsorption isotherms linear forms and fitted parameters

Isotherm type	Equation	R^2
Henry	$q_e = K_{HE}C_e$	0.775
Langmuir	$\frac{1}{q_e} = \frac{1}{K_L C_e Q_0} + \frac{1}{Q_0}$	0.995
Freundlich	$\log q_e = \log K_F + n \log C_e$	0.908
Temkin	$q_e = \frac{RT}{b_T} \ln A_T + \frac{RT}{b_T} \ln C_e$	0.489
Dubinin–Radushkevich	$\ln q_e = q_s - K_{D-R} \varepsilon^2$	0.931

Table 2
Comparison of different adsorbents for dyes removal

Adsorbent	Adsorption time (min)	Dyes	Removal efficiency (%)	Reference
FeNi ₃ /SiO ₂ /TiO ₂	90	Humic acid	94.4	[25]
Shaddock peels-based activated carbon	150	Methyl orange	54.25	[26]
Peels of Watermelon	25	Eosin	79	[27]
Activated carbon	80	Methyl red	61	[28]
Chitosan/rectorite/carbon nanotubes composite foams	2,880	Methyl orange	80.5	[29]
MSM	21	Methyl orange	86.44	This work

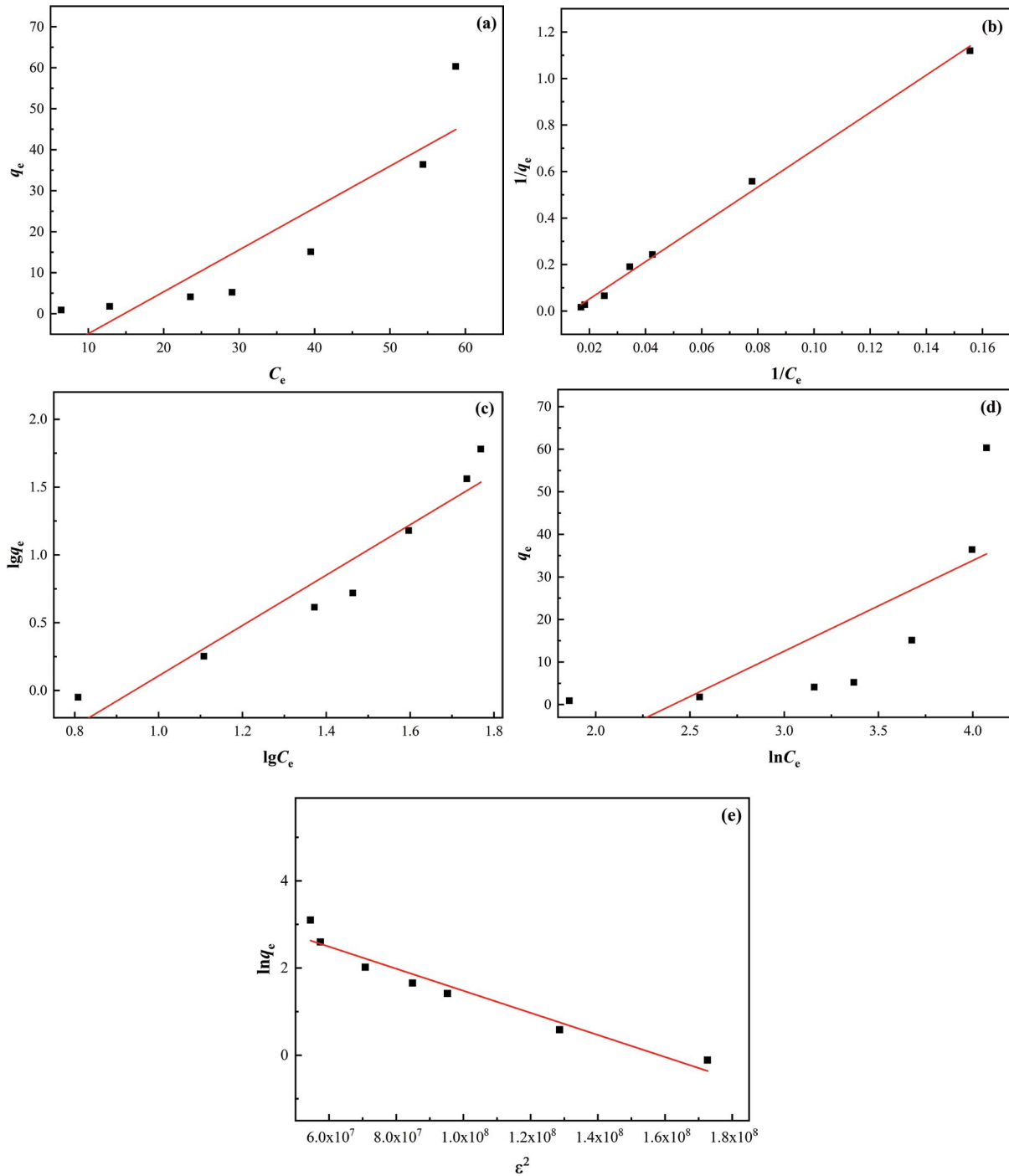


Fig. 7. Adsorption isotherms of MSM for methyl orange: (a) Henry, (b) Langmuir, (c) Freundlich, (d) Temkin, and (e) Dubinin-Radushkevich).

adsorption sites was linearly related to the amounts of unattached adsorption sites. The premise of the quasi-second-order kinetic equation was that the adsorption rate was determined by the square of the amounts of adsorption sites on the surface of the unattached adsorbent.

Quasi-first-order kinetic equation as follows [32]:

$$\log(q_e - q_t) = \log q_e - k_1 t \tag{3}$$

Quasi-second-order kinetic equation as follows [32]:

$$\frac{t}{q_t} = \frac{1}{k_2 q_e^2} + \frac{t}{q_e} \tag{4}$$

As can be seen from Fig. 8, the fitting coefficient of the quasi-second-order kinetic model for the adsorption of methyl orange by MSM was $R^2 = 0.999$, which was greater

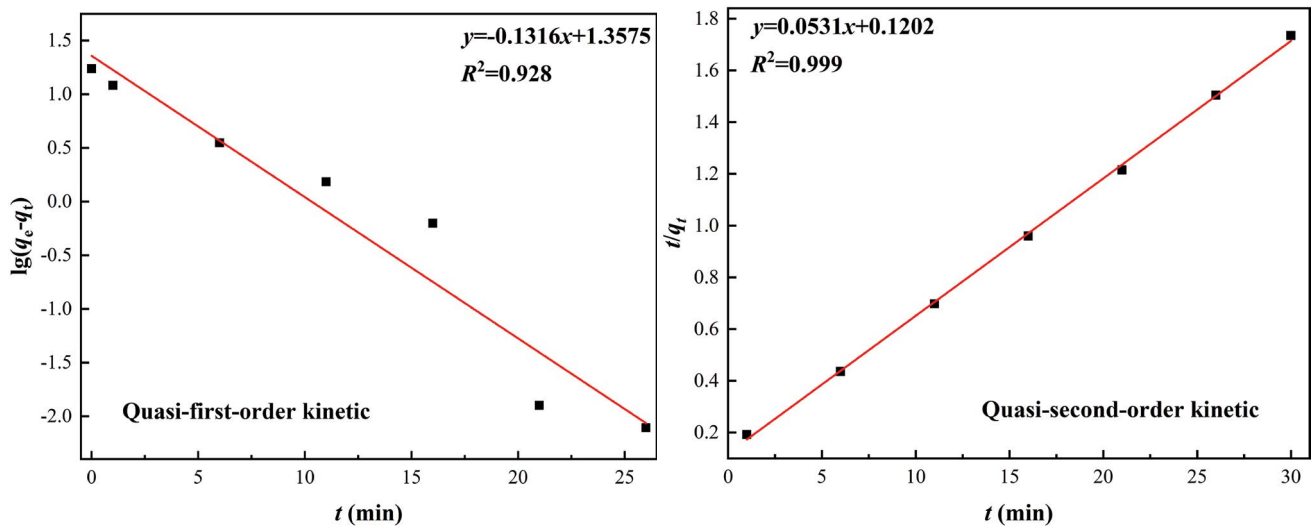


Fig. 8. Adsorption kinetic equation of MSM for methyl orange.

than the fitting coefficient of the quasi-first-order kinetic model ($R^2 = 0.928$). Therefore, the quasi-second-order kinetic model in this paper could be well described the adsorption process of methyl orange by MSM, indicating that chemical adsorption was the main step for MSM adsorbed methyl orange, which was consistent with the adsorption isotherm characterization results.

3.3.3. Adsorption thermodynamics

The adsorption thermodynamics was analyzed to further investigate the adsorption process of methyl orange by MSM. The thermodynamic parameters such as standard Gibbs free energy (ΔG°), enthalpy (ΔH°) and entropy (ΔS°) of the adsorption process were calculated by the following equations [37,38].

$$\Delta G^\circ = \Delta H^\circ - T\Delta S^\circ \quad (5)$$

$$\Delta G^\circ = -RT \ln K_c \quad (6)$$

$$K_c = \frac{Q_e}{C_e} \quad (7)$$

where R is the universal gas constant; T is the adsorption temperature; K_c is the equilibrium constant of the adsorption; Q_e and C_e are the equilibrium concentration of the methyl orange on adsorbent and in solution, respectively. Combined with Eqs. (5)–(7), the following linear equations can be inferred.

$$\ln \frac{Q_e}{C_e} = \frac{\Delta S^\circ}{R} - \frac{\Delta H^\circ}{RT} \quad (8)$$

The linear plot of $\ln Q_e/C_e$ vs. $1/T$ based on the experimental is shown in Fig. 9, the slope and intercept of which gives ΔH° and ΔS° . The thermodynamic parameters at different temperatures are listed in Table 4. As we all know,

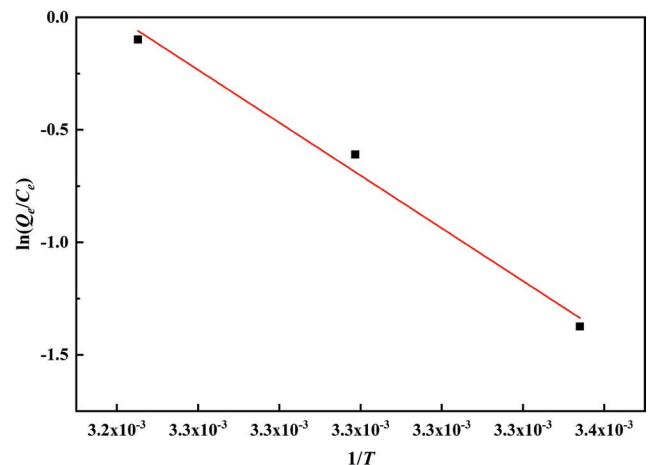


Fig. 9. Calculation of thermodynamic parameters for the adsorption of methyl orange on MSM.

the positive value of ΔG° indicates that the adsorption process is non-spontaneous, the positive value of ΔH° indicates that the adsorption phenomenon is endothermic; and vice versa. In this case, a positive ΔG° value indicated that the adsorption process was non-spontaneous, and the system energy obtained from an external source. Moreover, a positive ΔH° value indicated that adsorption was endothermic, and the positive ΔS° value indicated an increase in the degree of freedom, that is, the disorderly arrangement of molecules at the interface of the adsorbent solution.

3.3.4. Possible adsorption mechanism

The adsorption isotherm, kinetic and thermodynamic parameters of the adsorption of methyl orange by MSM were analyzed based on the experimental data. It was inferred that the above adsorption process was favorable chemical adsorption. Furthermore, in the acidic methyl

Table 4
Thermodynamic parameters for the adsorption of methyl orange on MSM

T (K)	lnK _c	ΔG° (kJ/mol)	ΔH° (kJ/mol)	ΔS° (kJ/mol/K)
298.15	-1.374	3.407	97.516	0.316
303.15	-0.610	1.538		
308.15	-0.099	0.254		

orange solution, the difference between the concentration of H⁺ or H₃O⁺ on the surface of MSM and in the solution promotes the protonation of the surface of MSM, which made the surface of MSM with positive charge. Methyl orange as a typical anionic dye, and the strong electrostatic attraction of anions and cations was considered to be the most important interaction force for the adsorption of methyl orange [39]. On the other hand, there was a large amount of Si-OH on the surface of MSM, which may combine with N atoms on methyl orange to form hydrogen bond interaction. Besides, the possibility of the *n*-π stacking interaction between the lone pair electrons on the oxygen atom and the π orbital of the dye aromatic ring should also be taken into account [40]. Hence, the adsorption mechanism in this paper may be described by electrostatic interaction, hydrogen bond interaction, and *n*-π stacking interaction.

4. Conclusions

In this paper, the MSM adsorbent was successfully performed via the sol-gel method between TEOS and F127. The effects of pH, dosage of MSM, temperature and time on dyeing wastewater decolorization efficiency simulated by methyl orange were investigated. Five adsorption isotherm models, kinetics, thermodynamics, and mechanism of the adsorption process were also discussed in detail. The results presented that the MSM with a large surface area was successfully prepared after calcined. The optimal adsorption conditions were that the pH of methyl orange solution was 1, the adsorbent dosage as 0.25 g, the adsorption temperature and time of 40°C and 21 min. Under the optimum conditions, the adsorption rate reached 86.44%. The adsorption process of methyl orange by MSM was indicated as a non-spontaneous monolayer favorable chemical adsorption process, which obeyed the pseudo-second-order kinetic model. The above showed that the MSM adsorbent with fast adsorption rate and high efficiency was synthesized by a simple preparation and mild condition method, which provided a theoretical basis and technical support for the application of dyeing wastewater treatment. In future, high-quality adsorbents can be prepared by different adsorption methods to conduct a comparative analysis of adsorption performances, and to further improve the adsorption capacity, making it a promising adsorbent for wastewater treatment.

Acknowledgment

This work was financially supported by the National Key R&D Program of China (2017YFB0304300&2017YFB0304303).

References

- [1] Y. Jin, G.J. Gan, X.Y. Yu, D.D. Wu, L. Zhang, N. Yang, J.D. Hu, Z.H. Liu, L.X. Zhang, H.C. Hong, X.Q. Yan, Y. Liang, L.X. Ding, Y.L. Pan, Isolation of viable but non-culturable bacteria from printing and dyeing wastewater bioreactor based on resuscitation promoting factor, *Curr. Microbiol.*, 74 (2017) 787–797.
- [2] C.-L. Zhang, R.-H. Ma, M.-R. Yang, R. Cao, Q. Wen, Synthesis, characterization, and photocatalytic performance of a ternary composite catalyst α-SiW₁₁Cr/PANI/ZnO, *J. Coord. Chem.*, 73 (2020) 229–242.
- [3] J.Y. Liang, X.-A. Ning, M.Y. Kong, D.H. Liu, G.W. Wang, H. Cai, J. Sun, Y.P. Zhang, X.W. Lu, Y. Yuan, Elimination and ecotoxicity evaluation of phthalic acid esters from textile-dyeing wastewater, *Environ. Pollut.*, 231 (2017) 115–122.
- [4] K. Piaskowski, R. Świdzka-Dąbrowska, P.K. Zarzycki, Dye removal from water and wastewater using various physical, chemical, and biological processes, *J. AOAC Int.*, 101 (2018) 1371–1384.
- [5] H.F. Wu, S.H. Wang, H.L. Kong, T.T. Liu, M.F. Xia, Performance of combined process of anoxic baffled reactor-biological contact oxidation treating printing and dyeing wastewater, *Bioresour. Technol.*, 98 (2007) 1501–1504.
- [6] S. Ledakowicz, M. Solecka, R. Zylla, Biodegradation, decolourisation and detoxification of textile wastewater enhanced by advanced oxidation processes, *J. Biotechnol.*, 89 (2001) 175–184.
- [7] F. Ramezani, R. Zare-Dorabei, Simultaneous ultrasonic-assisted removal of malachite green and methylene blue from aqueous solution by Zr-SBA-15, *Polyhedron*, 166 (2019) 153–161.
- [8] H. Ma, S.Y. Pu, Y.Q. Hou, R.X. Zhu, A. Zinchenko, W. Chu, A highly efficient magnetic chitosan “fluid” adsorbent with a high capacity and fast adsorption kinetics for dyeing wastewater purification, *Chem. Eng. J.*, 345 (2018) 556–565.
- [9] G.Z. Kyzas, J. Fu, K.A. Matis, The change from past to future for adsorbent materials in treatment of dyeing wastewaters, *Materials*, 6 (2013) 5131–5158.
- [10] E. Errais, J. Duplay, F. Darragi, Textile dye removal by natural clay – case study of Fouchana Tunisian clay, *Environ. Technol.*, 31 (2010) 373–380.
- [11] M.S. Tehrani, R. Zare-Dorabei, Competitive removal of hazardous dyes from aqueous solution by MIL-68(Al): derivative spectrophotometric method and response surface methodology approach, *Spectrochim. Acta, Part A*, 160 (2016) 8–18.
- [12] E. Zanin, J. Scapinello, M. de Oliveira, C.L. Rambo, F. Francescon, L. Freitas, J.M. Muneron de Mello, M.A. Fiori, J. Vladimir Oliveira, J. Dal Magro, Adsorption of heavy metals from wastewater graphic industry using clinoptilolite zeolite as adsorbent, *Process Saf. Environ. Prot.*, 105 (2017) 194–200.
- [13] H. Wu, Z.Z. Liu, A.M. Li, H. Yang, Evaluation of starch-based flocculants for the flocculation of dissolved organic matter from textile dyeing secondary wastewater, *Chemosphere*, 174 (2017) 200–207.
- [14] R. Kamaraj, A. Pandiarajan, M.R. Gandhi, A. Shibayama, S. Vasudevan, Eco-friendly and easily prepared graphene nanosheets for safe drinking water: removal of chlorophenoxyacetic acid herbicides, *ChemistrySelect*, 2 (2017) 342–355.
- [15] A. Pandiarajan, R. Kamaraj, S. Vasudevan, S. Vasudevan, OPAC (orange peel activated carbon) derived from waste orange peel for the adsorption of chlorophenoxyacetic acid herbicides from water: adsorption isotherm, kinetic modelling and thermodynamic studies, *Bioresour. Technol.*, 261 (2018) 329–341.
- [16] L. Huang, J. Liu, F. Gao, Q. Cheng, B. Lu, H. Zheng, H.X. Xu, P.H. Xu, X.Z. Zhang, X. Zeng, A dual-responsive, hyaluronic acid targeted drug delivery system based on hollow mesoporous silica nanoparticles for cancer therapy, *J. Mater. Chem. B*, 6 (2018) 4618–4629.
- [17] S. Schlichter, M. Rocha, A.F. Peixoto, J. Pires, C. Freire, M. Alvarez, Copper mesoporous materials as highly efficient

- recyclable catalysts for the reduction of 4-nitrophenol in aqueous media, *Polyhedron*, 150 (2018) 69–76.
- [18] C. Thörn, H. Gustafsson, L. Olsson, Immobilization of feruloyl esterases in mesoporous materials leads to improved transesterification yield, *J. Mater. Chem. B*, 72 (2011) 57–64.
- [19] R. Malik, P.S. Rana, V.K. Tomer, V. Chaudhary, S.P. Nehra, S. Duhhan, Nano gold supported on ordered mesoporous WO₃/SBA-15 hybrid nanocomposite for oxidative decolorization of azo dye, *Microporous Mesoporous Mater.*, 225 (2016) 245–254.
- [20] T. Yamaguchi, M. Ogawa, Hydrophilic internal pore and hydrophobic particle surface of organically modified mesoporous silica particle to host photochromic molecules, *Chem. Lett.*, 48 (2019) 170–172.
- [21] A. Mehdinia, S. Shegefti, F. Shemirani, Removal of lead(II), copper(II) and zinc(II) ions from aqueous solutions using magnetic amine-functionalized mesoporous silica nanocomposites, *J. Braz. Chem. Soc.*, 26 (2015) 2249–2257.
- [22] J.Z. Guo, S.W. Chen, L. Liu, B. Li, P. Yang, L.J. Zhang, Y.L. Feng, Adsorption of dye from wastewater using chitosan-CTAB modified bentonites, *J. Colloid Interface Sci.*, 382 (2012) 61–66.
- [23] X.F. Zhang, X.L. Dong, H. Huang, B. Lv, X.G. Zhu, J.P. Lei, S. Ma, W. Liu, Z.D. Zhang, Synthesis, structure and magnetic properties of SiO₂-coated Fe nanocapsules, *Mater. Sci. Eng., A*, 454 (2007) 211–215.
- [24] S. Nourozi, R. Zare-Dorabei, Highly efficient ultrasonic-assisted removal of methylene blue from aqueous media by magnetic mesoporous silica: experimental design methodology, kinetic and equilibrium studies, *Desal. Water Treat.*, 85 (2017) 184–196.
- [25] F. Akbari, M. Khodadadi, A. Hossein Panahi, A. Naghizadeh, Synthesis and characteristics of a novel FeNi₃/SiO₂/TiO₂ magnetic nanocomposites and its application in adsorption of humic acid from simulated wastewater: study of isotherms and kinetics, *Environ. Sci. Pollut. Res.*, 26 (2019) 32385–32396.
- [26] X.M. Tao, Y.H. Wu, L.G. Cha, Shaddock peels-based activated carbon as cost-saving adsorbents for efficient removal of Cr(VI) and methyl orange, *Environ. Sci. Pollut. Res.*, 26 (2019) 19828–19842.
- [27] S. Latif, R. Rehman, M. Imran, S. Iqbal, A. Kanwal, L. Mitu, Removal of acidic dyes from aqueous media using *Citrullus lanatus* peels: an agrowaste-based adsorbent for environmental safety, *J. Chem.*, 2019 (2019) 1–10.
- [28] E.A. Khan, Shahjahan, T.A. Khan, Adsorption of methyl red on activated carbon derived from custard apple (*Annona squamosa*) fruit shell: equilibrium isotherm and kinetic studies, *J. Mol. Liq.*, 249 (2018) 1195–1211.
- [29] J.J. Chen, X.W. Shi, Y.F. Zhan, X.D. Qiu, Y.M. Du, H.B. Deng, Construction of horizontal stratum landform-like composite foams and their methyl orange adsorption capacity, *Appl. Surf. Sci.*, 397 (2017) 133–143.
- [30] M.A. Al-Ghouti, D.A. Da'ana, Guidelines for the use and interpretation of adsorption isotherm models: a review, *J. Hazard. Mater.*, 393 (2020) 122383, <https://doi.org/10.1016/j.jhazmat.2020.122383>.
- [31] J.L. Wang, X. Guo, Adsorption isotherm models: classification, physical meaning, application and solving method, *Chemosphere*, 258 (2020) 127279, <https://doi.org/10.1016/j.chemosphere.2020.127279>.
- [32] R. Kamaraj, S. Vasudevan, Facile one-pot synthesis of nano-zinc hydroxide by electro-dissolution of zinc as a sacrificial anode and the application for adsorption of Th⁴⁺, U⁴⁺, and Ce⁴⁺ from aqueous solution, *Res. Chem. Intermed.*, 42 (2016) 4077–4095.
- [33] R. Kamaraj, D.J. Davidson, G. Sozhan, S. Vasudevan, Adsorption of herbicide 2-(2,4-dichlorophenoxy)propanoic acid by electrochemically generated aluminum hydroxides: an alternative to chemical dosing, *RSC Adv.*, 5 (2015) 39799–39809.
- [34] A. Özcan, A.S. Özcan, S. Tunalı, T. Akar, I. Kiran, Determination of the equilibrium, kinetic and thermodynamic parameters of adsorption of copper(II) ions onto seeds of *Capsicum annuum*, *J. Hazard. Mater.*, 124 (2005) 200–208.
- [35] M.S. Onyango, Y. Kojima, O. Aoyi, E.C. Bernardo, H. Matsuda, Adsorption equilibrium modeling and solution chemistry dependence of fluoride removal from water by trivalent-cation-exchanged zeolite F-9, *J. Colloid Interface Sci.*, 279 (2004) 341–350.
- [36] M. Chabani, A. Amrane, A. Bensmaili, Kinetic modelling of the adsorption of nitrates by ion exchange resin, *Chem. Eng. J.*, 125 (2006) 111–117.
- [37] A.S. Manchaiah, V. Badalamoole, Novel heterocyclic chitosan-based Schiff base: evaluation as adsorbent for removal of methyl orange from aqueous solution, *Water Environ. J.*, 34 (2020) 364–373.
- [38] R. Kamaraj, A. Pandiarajan, S. Jayakiruba, Mu. Naushad, S. Vasudevan, Kinetics, thermodynamics and isotherm modeling for removal of nitrate from liquids by facile one-pot electrosynthesized nano zinc hydroxide, *J. Mol. Liq.*, 215 (2016) 204–211.
- [39] N.N. Bahrudin, M.A. Nawı, A.H. Jawad, S. Sabar, Adsorption characteristics and mechanistic study of immobilized chitosan-montmorillonite composite for methyl orange removal, *J. Polym. Environ.*, 28 (2020) 1901–1913.
- [40] A.H. Jawad, N.F.H. Mamat, B.H. Hameed, K. Ismail, Biofilm of cross-linked chitosan-ethylene glycol diglycidyl ether for removal of Reactive Red 120 and methyl orange: adsorption and mechanism studies, *J. Environ. Chem. Eng.*, 7 (2019) 102965, <https://doi.org/10.1016/j.jece.2019.102965>.